

1   **Magnitude and uncertainty of nitrous oxide emissions from North America based on**  
2   **bottom-up and top-down approaches: Informing future research and national**  
3   **inventories**

4   R. Xu<sup>1,2</sup>, H. Tian<sup>1</sup>, N. Pan<sup>1</sup>, R. L. Thompson<sup>3</sup>, J. G. Canadell<sup>4</sup>, E. A. Davidson<sup>5</sup>, C. Nevison<sup>6</sup>, W.  
5   Winiwarter<sup>7,8</sup>, H. Shi<sup>1</sup>, S. Pan<sup>1</sup>, J. Chang<sup>9</sup>, P. Ciais<sup>10</sup>, S. R. S. Dangal<sup>11</sup>, A. Ito<sup>12</sup>, R. B. Jackson<sup>13</sup>,  
6   F. Joos<sup>14</sup>, R. Lauerwald<sup>15</sup>, S. Lienert<sup>14</sup>, T. Maavara<sup>16</sup>, D. B. Millet<sup>17</sup>, P. A. Raymond<sup>16</sup>, P.  
7   Regnier<sup>18</sup>, F. N. Tubiello<sup>19</sup>, N. Vuichard<sup>10</sup>, K. C. Wells<sup>17</sup>, C. Wilson<sup>20,21</sup>, J. Yang<sup>22</sup>, Y. Yao<sup>1</sup>, S.  
8   Zaehle<sup>23</sup>, F. Zhou<sup>24</sup>

9  
10   <sup>1</sup>International Center for Climate and Global Change Research, School of Forestry and Wildlife  
11   Sciences, Auburn University, Auburn, AL, USA.

12   <sup>2</sup>Forest Ecosystems and Society, Oregon State University, Corvallis, OR, USA.

13   <sup>3</sup>Norsk Institutt for Luftforskning, NILU, Kjeller, Norway.

14   <sup>4</sup>Global Carbon Project, CSIRO Oceans and Atmosphere, Canberra, Australia.

15   <sup>5</sup>Appalachian Laboratory, University of Maryland Center for Environmental Science, Frostburg, MD,  
16   USA.

17   <sup>6</sup>University of Colorado Boulder/INSTAAR, Boulder, CO, USA.

18   <sup>7</sup>International Institute for Applied Systems Analysis, Laxenburg, Austria.

19   <sup>8</sup>Institute of Environmental Engineering, University of Zielona Góra, Zielona Góra, Poland.

20   <sup>9</sup>College of Environmental and Resource Sciences, Zhejiang University, Hangzhou, China.

21   <sup>10</sup>Laboratoire des Sciences du Climat et de l'Environnement, LSCE, CEA CNRS, UVSQ  
22   UPSACLAY, Gif sur Yvette, France.

23   <sup>11</sup>School of Natural Resources, University of Nebraska – Lincoln, NE, USA.

24   <sup>12</sup>Earth System Division, National Institute for Environmental Studies, Tsukuba, Japan.

25   <sup>13</sup>Department of Earth System Science, Woods Institute for the Environment, and Precourt Institute  
26   for Energy, Stanford University, Stanford, CA, USA.

27   <sup>14</sup>Climate and Environmental Physics, Physics Institute and Oeschger Centre for Climate Change  
28   Research, University of Bern, Bern, Switzerland.

29   <sup>15</sup>Université Paris-Saclay, INRAE, AgroParisTech, UMR ECOSYS, Thiverval-Grignon, France.

30   <sup>16</sup>Yale School of Forestry and Environmental Studies, New Haven, CT, USA.

31   <sup>17</sup>Department of Soil, Water, and Climate, University of Minnesota, MN, USA.

32   <sup>18</sup>Department Geoscience, Environment & Society-BGEOSYS, Université Libre de Bruxelles,  
33   Brussels, Belgium.

34   <sup>19</sup>Statistics Division, Food and Agriculture Organization of the United Nations, Via Terme di  
35   Caracalla, Rome, Italy.

36   <sup>20</sup>National Centre for Earth Observation, University of Leeds, Leeds, UK.

37   <sup>21</sup>Institute for Climate and Atmospheric Science, School of Earth and Environment, University of  
38   Leeds, Leeds, UK.

39   <sup>22</sup>Department of Forestry, Mississippi State University, Mississippi State, MS, USA.

40   <sup>23</sup>Max Planck Institute for Biogeochemistry, Jena, Germany.

41   <sup>24</sup>Sino-France Institute of Earth Systems Science, Laboratory for Earth Surface Processes, College of  
42   Urban and Environmental Sciences, Peking University, Beijing, China.

43   Corresponding author: Hanqin Tian ([tianhan@auburn.edu](mailto:tianhan@auburn.edu))

44      **Key Points:**

- 45      • The total N<sub>2</sub>O emissions over North America during 2007–2016 are estimated at  
46      0.9–3.0 Tg N yr<sup>-1</sup> using a combination of bottom-up and top-down approaches.
- 47      • North American anthropogenic N<sub>2</sub>O emissions grew by ~0.2 Tg N during 1980–2016;  
48      U.S. agriculture was the largest cause of that growth.
- 49      • Modeled N<sub>2</sub>O fluxes in this study reflect an IPCC tier 3 approach, and can improve GHG  
50      inventories that largely use tier 1 approaches.

51

52 **Abstract**

53 We synthesized N<sub>2</sub>O emissions over North America using 17 bottom-up (BU) estimates from  
 54 1980–2016 and five top-down (TD) estimates from 1998–2016. The BU-based total emission  
 55 shows a slight increase owing to U.S. agriculture, while no consistent trend is shown in TD  
 56 estimates. During 2007–2016, North American N<sub>2</sub>O emissions are estimated at 1.7 (1.0–3.0) Tg  
 57 N yr<sup>-1</sup> (BU) and 1.3 (0.9–1.5) Tg N yr<sup>-1</sup> (TD). Anthropogenic emissions were twice larger than  
 58 natural fluxes from soil and water. Direct agricultural and industrial activities accounted for 68%  
 59 of total anthropogenic emissions, 71% of which was contributed by the U.S. Our estimates of  
 60 U.S. agricultural emissions are comparable to the EPA greenhouse gas (GHG) inventory, which  
 61 includes estimates from IPCC tier 1 (emission factor) and tier 3 (process-based modeling)  
 62 approaches. Conversely, our estimated agricultural emissions for Canada and Mexico are twice  
 63 as large as the respective national GHG inventories based on tier 1 approaches.

64

65 **Plain Language Summary**

66 Nitrous oxide (N<sub>2</sub>O) is the third most important greenhouse gases (GHGs) after CO<sub>2</sub> and CH<sub>4</sub>  
 67 causing global warming. Among world regions, North America (defined herein as U.S., Canada,  
 68 and Mexico) is the second largest source of N<sub>2</sub>O emissions globally, and previous source  
 69 estimates for this region vary widely. This study aims to provide a comprehensive N<sub>2</sub>O  
 70 assessment over North America including all available estimates based on a number of  
 71 approaches. We report total emissions, and emissions from four anthropogenic source sectors,  
 72 over the past four decades. Agriculture and industry are two major N<sub>2</sub>O sources in North  
 73 America. Our results show a minor increase in the total N<sub>2</sub>O emission due to agricultural trends  
 74 in the U.S. Our bottom-up estimate of U.S. agricultural N<sub>2</sub>O emissions are close to those in the  
 75 EPA national GHG inventory that includes both empirical and modeled results. The high  
 76 consistency suggests the need to take process-based modeling results into account for future  
 77 national GHG inventories.

78

79 **1 Introduction**

80 Atmospheric nitrous oxide (N<sub>2</sub>O), the third most-important greenhouse gas (GHG) and a  
 81 key stratospheric ozone-depleting substance, has increased by 21% globally since 1750 due to  
 82 anthropogenic activities (Ciais et al., 2014; Prinn et al., 2018). North America is the second-  
 83 largest contributor to total global anthropogenic N<sub>2</sub>O emissions (Tian et al., 2020a)—a region  
 84 that consumed 16% of the world’s synthetic nitrogen (N) fertilizer (Lu & Tian, 2017; FAO,  
 85 2021), produced 9% of the world’s animal manure (Zhang et al., 2017; FAO, 2021), and received  
 86 16% of the world’s atmospheric N deposition from industrial and agricultural activities (Eyring  
 87 et al., 2013). An emission hot spot has also been observed in the Midwestern Corn Belt, one of  
 88 the most intensively managed agricultural areas in the world and which accounted for 30% of  
 89 total North American emissions during the period 2008–2014 (Nevison et al., 2018).

90 Bottom-up (BU; i.e., inventories and models) and top-down (TD; i.e., atmospheric  
 91 inversions) approaches represent the two primary methods for estimating global, regional and  
 92 country level emissions (Miller et al., 2012; Nevison et al., 2018; Saikawa et al., 2014; Shang et

93 al., 2019; Stehfest & Bouwman, 2006; Tian et al., 2016; Tian et al., 2020a; Wilson et al., 2014;  
94 X. Xu et al., 2012); a number of studies have estimated N<sub>2</sub>O emissions from North America  
95 based on both approaches. Yet considerable uncertainty remains in estimates of total and  
96 sectorial emissions. For example, it is a long-standing debate whether BU emission inventories  
97 may underestimate N<sub>2</sub>O emission over North America, especially in the Midwestern Corn Belt  
98 (Chen et al., 2016; Del Grosso et al., 2010; T. Griffis et al., 2013; Kort et al., 2008; Miller et al.,  
99 2012; Nevison et al., 2018). Moreover, current uncertainty in estimates of North American N<sub>2</sub>O  
100 emissions could be reduced by reconciling the TD inversions with BU calculations.

101 The present study synthesized available N<sub>2</sub>O emissions over North America [defined  
102 here as the region comprising the United States (U.S.), Canada, and Mexico] using 17 BU  
103 (emission inventories, spatial extrapolation of field flux measurements, nutrient budget  
104 modeling, and terrestrial biosphere models) and five TD estimates for the period 1980–2016  
105 (Figure S1). Data sources for all estimates are consistent with Tian et al. (2020a). We examined  
106 estimates of N<sub>2</sub>O emissions and the associated uncertainties for both approaches. In addition,  
107 national GHG emissions inventories developed by the U.S. (based on both Tier 1 and Tier 3  
108 methods), by Canada and Mexico (Tier 1)) were used to compare against the BU estimates in  
109 this study of national total and sectorial N<sub>2</sub>O emissions relative to the period 1990–2016.

## 110 2 Materials and Methods

### 111 2.1 Data Sources

#### 112 2.1.1 Bottom-up Estimates

113 We collected N<sub>2</sub>O emissions from 17 BU estimates. National N<sub>2</sub>O emissions from  
114 models and inventories include: six terrestrial biosphere models for natural and cropland soils  
115 with consideration of multiple environmental factors [Global N<sub>2</sub>O Model Inter-comparison  
116 Project (NMIP, Tian et al. (2019)); three Dynamic Land Ecosystem Model (DLEM)-only  
117 simulations [i.e., for pastures (Dangal et al., 2019), rivers and reservoirs (Yao et al., 2020), and  
118 biomass burning]; two mechanistic stochastic model simulations for the river-reservoir-estuary  
119 continuum (Maavara et al., 2019) and lakes (Lauerwald et al., 2019); three national GHG  
120 emissions inventories [EDGAR v4.3.2, Janssens-Maenhout et al. (2019); FAOSTAT, Tubiello  
121 (2019); GAINS, Winiwarter et al. (2018)]; one fire emissions database for biomass burning  
122 [GFED4s, Van Der Werf et al. (2017)]; one statistical model for cropland soils [SRNM, Wang et  
123 al. (2019)]; and one estimate of aquaculture emissions calculated based on quantified N flows  
124 from a nutrient budget model (Bouwman et al., 2013). Six terrestrial biosphere models  
125 participated in NMIP provided N<sub>2</sub>O emissions from natural and agricultural soils. All  
126 participating models were driven by consistent input datasets (i.e., climate, atmospheric CO<sub>2</sub>  
127 concentration, land cover change, atmospheric N deposition, mineral N fertilization, and manure  
128 N application) at the spatial resolution of 0.5° globally and covered the 1861–2016 period (Tian  
129 et al., 2019). Model-based estimates of national N flows (i.e., fish feed intake, fish harvest, and  
130 waste) in freshwater and marine aquaculture were obtained from Beusen et al. (2016) and  
131 Bouwman et al. (2011, 2013). We then calculated aquaculture N<sub>2</sub>O emissions by considering  
132 1.8% loss of N waste in aquaculture, the same EF used in MacLeod et al. (2019). EF  
133 uncertainties of aquaculture N<sub>2</sub>O range from 0.5% (IPCC, 2006) to 5% (Williams & Crutzen,

134 2010). A detailed description of each BU method was documented in the Supplementary  
135 Information of Tian et al. (2020a).

136 Anthropogenic N<sub>2</sub>O emissions have been reported annually by Annex I Parties to the  
137 United Nations Framework Convention on Climate Change (UNFCCC) for nearly thirty years,  
138 currently covering the period 1990–2019. More recently, also the other signatories to the  
139 UNFCCC have been requested to provide information on their national greenhouse gas  
140 inventories as a Biannual Update Report, with sufficient detail and transparency to track progress  
141 towards their nationally determined contributions. In this study, we obtained time-series  
142 anthropogenic N<sub>2</sub>O emissions from the most recent UNFCCC reporting that was submitted by  
143 the U.S. (Annex I Party; EPA GHG inventory, <https://unfccc.int/documents/272415>), Canada  
144 (Annex I Party; Canadian GHG inventory, <https://unfccc.int/documents/271493>), and Mexico  
145 (Non-Annex I Party; Mexican GHG inventory, <https://unfccc.int/documents/199243>) to compare  
146 with our estimates.

#### 147 2.1.2 Top-down Estimates

148 We include five estimates from four independent atmospheric inversion frameworks for  
149 the 1998–2016 period [INVICAT, Wilson et al. (2014); PyVAR-CAMS, Thompson et al.  
150 (2014); MIROC4-ACTM, Patra et al. (2018); and GEOSChem, Wells et al. (2015)], all of which  
151 used the Bayesian inversion method. Here, two versions of PyVAR-CAMS were run to  
152 determine the sensitivity of results to the prior estimate of ocean fluxes. These runs using high  
153 and low ocean priors are denoted as PyVAR-CAMS-1 and PyVAR-CAMS-2, respectively. For  
154 analyzing TD estimates over North America, we interpolated the coarser resolution results into  
155 0.5° × 0.5° over all land areas in the four frameworks (see Table S19 in Tian et al. (2020a)). A  
156 detailed description of each TD approach was documented in Supplementary Information of Tian  
157 et al. (2020a).

#### 158 2.2 Data Synthesis

159 BU approaches give N<sub>2</sub>O emissions estimates for five source categories, while TD  
160 approaches only provide total gridded emissions. BU estimates consist of N<sub>2</sub>O emissions from  
161 natural sources (i.e., ‘Natural soil baseline’ and natural emissions from inland water and  
162 estuaries), and from 12 anthropogenic sub-categories that were combined and further re-  
163 classified into four categories (Table 1, Figure S1): i) ‘Perturbed fluxes from climate/CO<sub>2</sub>/land  
164 cover change’ covering the CO<sub>2</sub> effect, climate effect, post-deforestation pulse effect, and long-  
165 term effect of reduced mature forest area, ii) ‘Direct emissions of N additions in the agricultural  
166 sector (Agriculture)’ covering direct application of synthetic N fertilizers and manure (direct soil  
167 emissions), manure left on pasture, manure management, and aquaculture, iii) ‘Indirect  
168 emissions from anthropogenic N additions’ covering atmospheric N deposition (NDEP) on land,  
169 and effects of anthropogenic loads of reactive N in inland waters and estuaries, and iv) ‘Other  
170 direct anthropogenic sources’ covering fossil fuel and industry, waste and waste water, and  
171 biomass burning. Here, ‘Natural soil baseline’ emissions reflect a situation without considering  
172 land use change (e.g., deforestation) and without considering anthropogenic N additions and  
173 indirect anthropogenic effects of environmental changes (i.e., climate, elevated CO<sub>2</sub>, and  
174 atmospheric N deposition). The four categories are aligned with the emission categories in the  
175 UNFCCC reporting and IPCC 2006 methodologies [see Table S14 in Tian et al. (2020a)].

176 **3 Results and Discussion**177 **3.1 BU and TD Estimates of Total N<sub>2</sub>O Emissions During 1980–2016**

178 BU and TD approaches diverge in the magnitude and trend of the total emission over  
 179 North America during 1980–2016 (Figure 1). In addition, larger uncertainties are derived for BU  
 180 estimates than for TD estimates, likely because the BU uncertainty is the sum of ranges  
 181 (minimum and maximum estimates) from 17 BU estimates with considerable contributions from  
 182 natural soils, agriculture, and the effects of climate and CO<sub>2</sub> (Table 1). During 1998–2016, the  
 183 BU estimate was 390 (70–1350) Gg N yr<sup>-1</sup> higher than the TD estimate, but the latter implied a  
 184 larger interannual variability (150 Gg N yr<sup>-1</sup>). The BU estimate demonstrated a steady increase at  
 185 a rate of 5±2 Gg N yr<sup>-1</sup> per year (95% confidence interval; P<0.05) during 1980–2016, while the  
 186 TD estimate decreased sharply between 1998 and 2005 and then started to increase again during  
 187 2006–2016, resulting in no significant overall trend. In the recent decade (2007–2016), North  
 188 American total N<sub>2</sub>O emissions were 1,680 (950–3,040) Gg N yr<sup>-1</sup> (BU) and 1,260 (910–1,510)  
 189 Gg N yr<sup>-1</sup> (TD) (Table 1). BU estimates for the U.S., Canada, and Mexico were 1,150 (690–  
 190 2110) Gg N yr<sup>-1</sup>, 270 (120–520) Gg N yr<sup>-1</sup>, and 260 (60–450) Gg N yr<sup>-1</sup>, respectively.

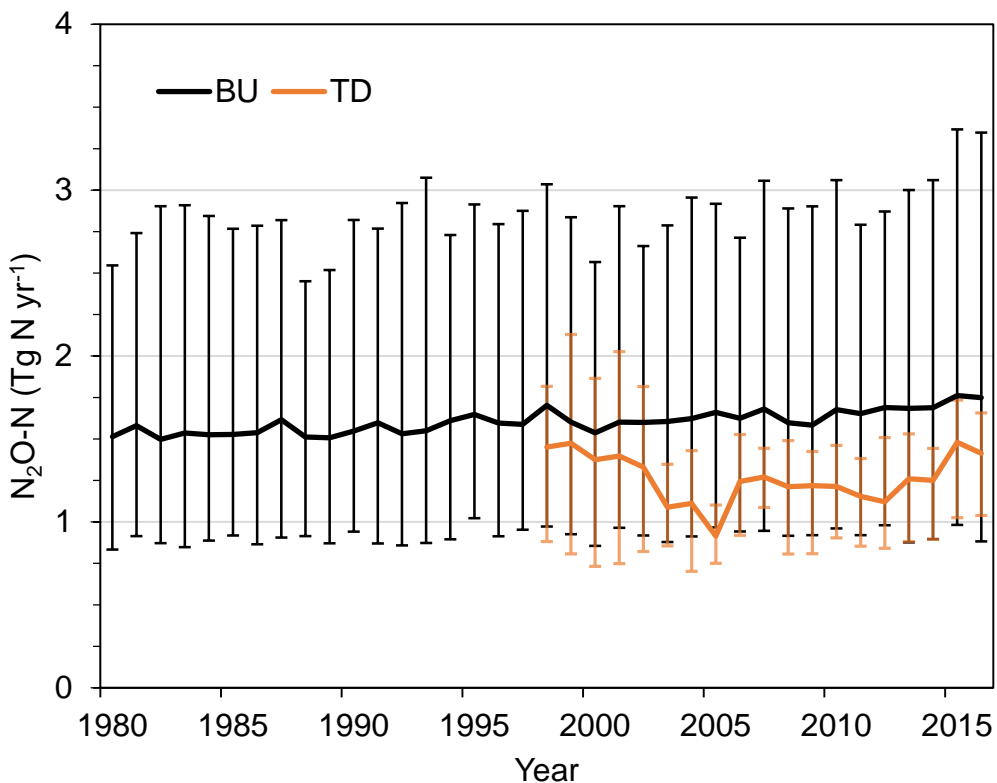
191  
 192 **Table 1.** N<sub>2</sub>O emission sources (expressed in Gg N yr<sup>-1</sup>) over North America (i.e., U.S., Canada,  
 193 and Mexico) during 2007–2016. All numbers are rounded to the nearest multiple of 10 for  
 194 sources >10 and nearest whole number for sources <10.

2007-2016			USA			Canada			Mexico			North America		
<i>Anthropogenic sources</i>			mean	min	max	mean	min	max	mean	min	max	mean	min	max
Direct emissions of N additions in the agricultural sector (Agriculture)	Direct soil emissions	300	180	620	40	20	60	30	10	70	370	220	730	
	Manure left on pasture	70	70	70	10	10	10	30	20	30	100	100	110	
	Manure management	20	10	20	0	0	10	10	0	10	30	10	30	
	Aquaculture	N/A	N/A	N/A	N/A	N/A	N/A	N/A	N/A	N/A	1	0	2	
	sub-total	390	260	710	50	30	80	70	30	110	500	330	870	
Other direct anthropogenic sources	Fossil fuel and industry	160	150	170	20	20	20	90	10	160	260	180	350	
	Waste and waste water	20	20	20	0	0	0	10	0	10	30	30	30	
	Biomass burning	20	10	40	30	10	60	0	0	0	60	30	100	
	sub-total	200	180	230	50	30	80	100	10	170	350	240	480	
Indirect emissions from anthropogenic N additions	Inland waters, estuaries, coastal zones	40	10	60	20	10	30	10	1	10	70	50	80	
	Atmospheric N deposition on land	80	30	240	10	10	30	10	10	20	110	50	280	
	sub-total	120	40	300	30	20	60	20	10	30	180	100	360	
Perturbed fluxes from climate/CO <sub>2</sub> /land cover change	Climate & CO <sub>2</sub> effect	40	-80	220	10	-30	50	-10	-20	3	40	-120	280	
	Post-deforestation pulse effect	120	120	120	10	10	10	10	10	20	140	140	150	
	Long-term effect of reduced mature forest area	-50	-50	-50	-10	-10	-10	-20	-20	-30	-80	-80	-80	
	sub-total	110	-10	290	10	-30	50	-20	-30	-10	100	-60	350	
Anthropogenic total			820	470	1,530	140	50	270	170	20	300	1,130	610	2,060
<i>Natural fluxes</i>														
Natural soils baseline			320	210	560	100	40	220	90	40	150	510	300	930
Natural (Inland waters, estuaries, coastal zones)			10	10	20	30	30	30	1	1	2	40	40	50
Natural total			330	220	580	130	70	250	90	40	150	550	340	980
<b>Bottom-up total source</b>			<b>1,150</b>	<b>690</b>	<b>2,110</b>	<b>270</b>	<b>120</b>	<b>520</b>	<b>260</b>	<b>60</b>	<b>450</b>	<b>1,680</b>	<b>950</b>	<b>3,040</b>
<b>Top-down total source</b>												<b>1,260</b>	<b>910</b>	<b>1,510</b>

195

196

197 Based on BU estimates, U.S. anthropogenic N<sub>2</sub>O emissions were 7% higher in  
 198 2007–2016 than in the 1980s, primarily because of a 27% increase in direct soil agricultural  
 199 emissions (Figure 2). In Mexico, total anthropogenic emissions are estimated to have increased  
 200 by 114%, due to a large yet quite uncertain contribution from industrial emissions over the most  
 201 recent decades, according to EDGAR v4.3.2 data (Figure 2; Table S1). By contrast,  
 202 anthropogenic emissions in Canada were relatively stable, with a slight increase in agricultural  
 203 emissions offset by a reduction in emissions from industrial activities. Natural soil emissions  
 204 were relatively constant in the three countries.



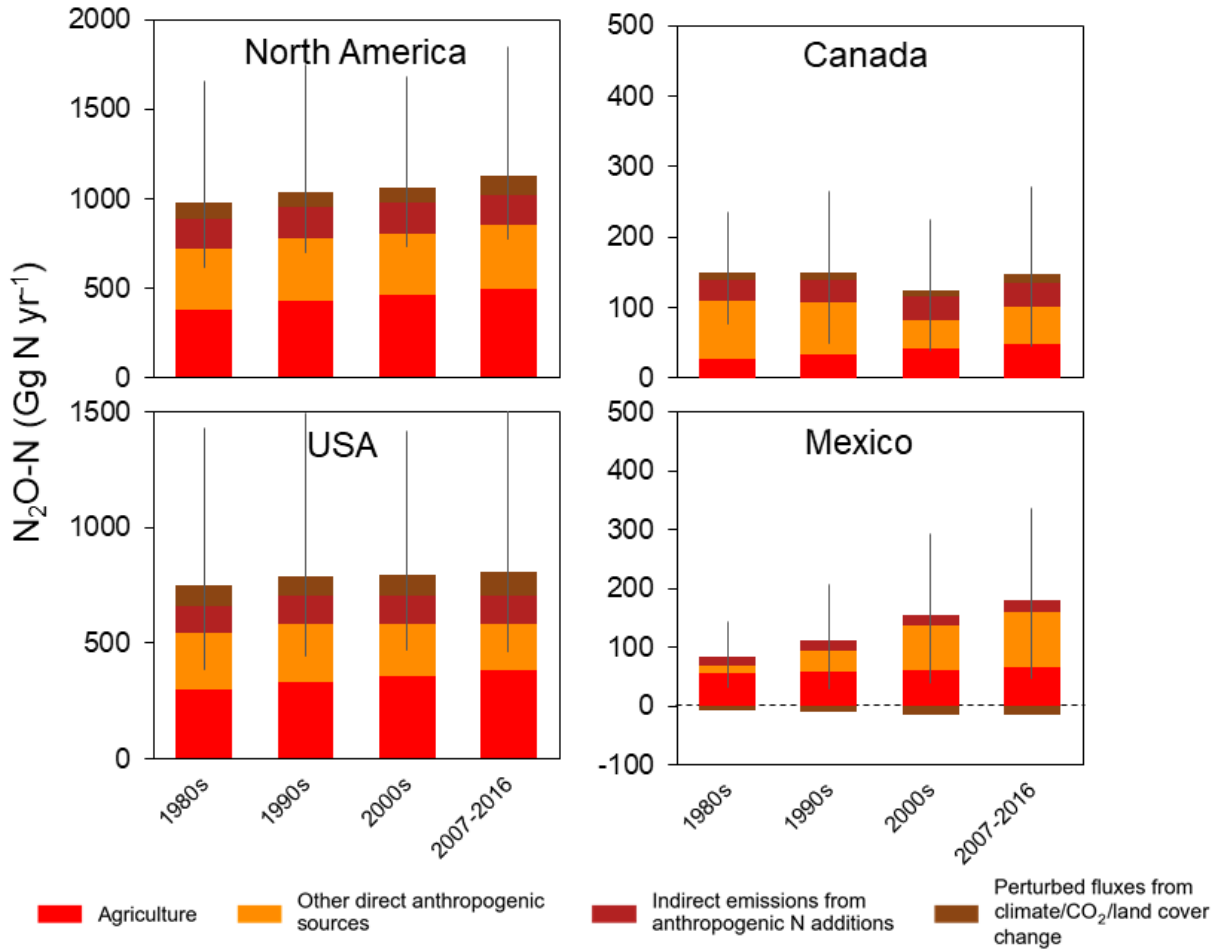
205

206 **Figure 1.** Comparison of annual total N<sub>2</sub>O emissions from North America estimated by BU  
 207 approaches during 1980–2016 and TD approaches during 1998–2016. Error bars indicate the  
 208 spread between the minimum and the maximum values.

### 209 3.2 BU Estimates of N<sub>2</sub>O Emissions Over 2007–2016

210 Two-thirds of total North American N<sub>2</sub>O emissions during 2007–2016 were linked to  
 211 anthropogenic sources, which averaged 1,120 Gg N yr<sup>-1</sup> versus 550 Gg N yr<sup>-1</sup> from natural  
 212 sources (Table 1). Among the anthropogenic emissions, agriculture (45%) was the largest  
 213 contributor, heavily dominated by direct soil emissions from synthetic N fertilizer and manure  
 214 application, followed by emissions associated with manure left on pasture in the U.S., reflecting  
 215 increased agricultural N inputs (Lu & Tian, 2017; Xu et al., 2019; FAO, 2021). Aquaculture  
 216 played a negligible role in North American N<sub>2</sub>O emissions. Direct soil emissions were the largest  
 217 agricultural source in all three countries, with fluxes in both Canada and Mexico about an order  
 218 of magnitude lower than those in the U.S (Figures S2-S4). Livestock manure-induced emissions  
 219 (i.e., manure left on pasture and manure management) were five times lower than direct soil

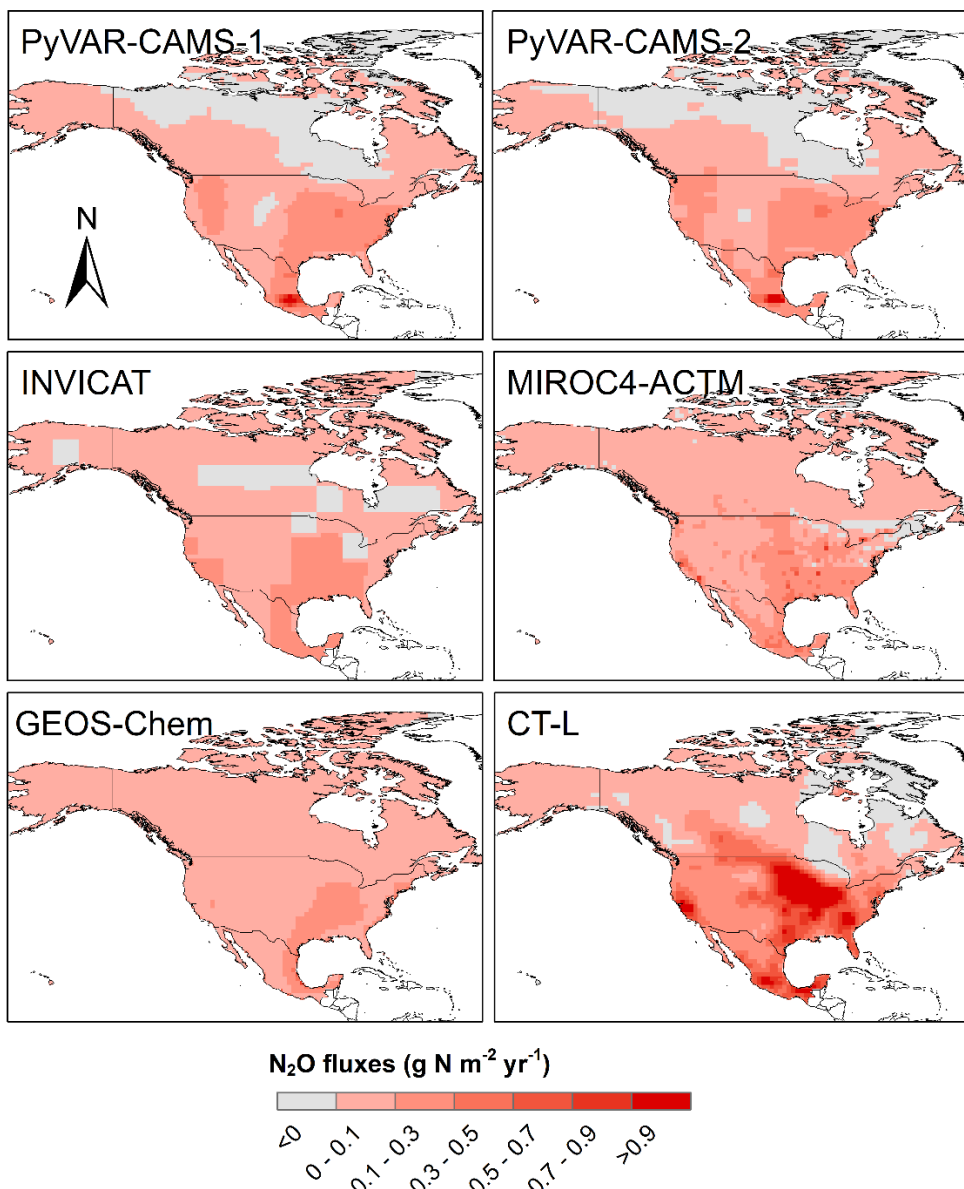
220 emissions in the U.S. and Canada, however, this source was comparable to direct agricultural soil  
 221 emissions in Mexico, where there has been a continuous increase in livestock numbers and  
 222 manure production since 1980 (FAO, 2020; Zhang et al., 2017).



223  
 224 **Figure 2.** Ensembles of anthropogenic N<sub>2</sub>O emissions over North America in the 1980s, 1990s,  
 225 2000s, and 2007–2016 based on BU approaches. Error bars indicate the spread between the  
 226 minimum and the maximum values of the total flux.

227 Other direct anthropogenic sources (31%) made up the second-largest contribution to  
 228 total continental emissions, and were primarily associated with emissions from fossil fuel and  
 229 industry in the U.S. and Mexico during 2007–2016 (Table 1). Biomass burning was another  
 230 important source of N<sub>2</sub>O but diverged across these three countries; such emissions in Canada  
 231 were twice and five times as high as in the U.S. and Mexico, respectively, between 2007 and  
 232 2016. Waste and waste water contributed least, with the largest share from the U.S. owing to its  
 233 large population (FAO, 2021). Indirect emissions due to anthropogenic N additions from NDEP  
 234 (110 Gg N yr<sup>-1</sup>) and mostly due to agricultural N leaching to inland and coastal waters (70 Gg N  
 235 yr<sup>-1</sup>) accounted for 15% of North American anthropogenic emissions during 2007–2016. Among  
 236 the three North American countries, the U.S. had the most intensive agricultural activities and  
 237 thus its indirect emissions were much higher than those from Canada and Mexico (Table 1).  
 238 Agricultural activity in the U.S., especially the Midwest, was the major driver for high indirect

239 emissions from NDEP (primarily ammonium) and leaching/runoff (primarily nitrate) from  
 240 synthetic N fertilizer and livestock manure (Chen et al., 2016; Du et al., 2016; Tian et al.,  
 241 2020b). We observed a considerable decline in NDEP-induced  $\text{N}_2\text{O}$  emissions from U.S. and  
 242 Canadian industrial activities due to enforcement of the amendments to the Clean Air Act in  
 243 1995, though this decline was overwhelmed by the effect of indirect emissions caused by N  
 244 losses from agriculture (Figures S2-S3). In contrast, Mexico showed a continuous increase in  
 245 indirect emissions from NDEP due to increases in both agricultural and industrial activities  
 246 (Figure S4).



247

248 **Figure 3.** Comparison of our total  $\text{N}_2\text{O}$  emissions by global inversion models with the estimate  
 249 by CT-L (Nevison et al., 2018) during 2008–2013. Global inversion models include PyVAR-  
 250 CAMS, INVICAT, MIROC4-ACTM, and GEOS-Chem.

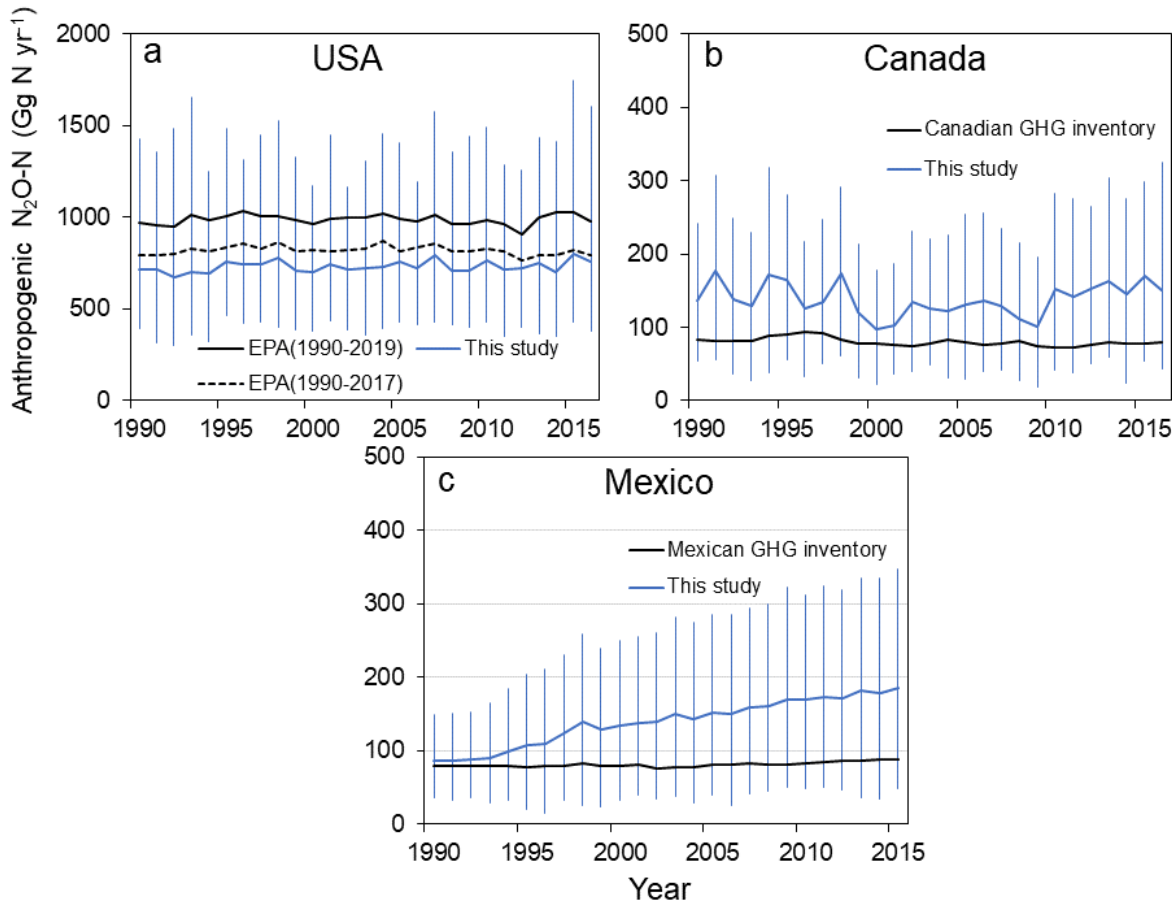
Perturbed fluxes caused by climate/CO<sub>2</sub>/land cover change contributed the least (9%) to total anthropogenic emissions over North America according to model simulations. The effects of climate and CO<sub>2</sub> accelerated soil N<sub>2</sub>O emissions with regional climate change. This has offset the reduction due to elevated CO<sub>2</sub> concentrations that enhance plant growth and associated N uptake and in turn decrease soil N<sub>2</sub>O emissions (Tian et al., 2019; Zaehle et al., 2011). The decrease in perturbed fluxes of soil N<sub>2</sub>O emissions over North America was only 80 Gg N yr<sup>-1</sup> (only 7% of the global reduction), because temperate forest soils generally have lower emissions than tropical forest soils and because the area of converted lands was much smaller than in the tropics (e.g., Amazon) between 2007 and 2016 (Hurt et al., 2011). This decrease can be balanced by the temporary rise of soil N<sub>2</sub>O emission after deforestation (post-deforestation pulse effect) plus background emissions from converted croplands or pastures (McDaniel et al., 2019; Meurer et al., 2016; van Lent et al., 2015; Verchot et al., 1999). In particular, within the U.S. the decrease in soil N<sub>2</sub>O emissions has been fully offset by the post-deforestation pulse effect, resulting in a positive increment of 60 Gg N yr<sup>-1</sup>; however, this was not the case in Mexico where only half of the emission decrease was counterbalanced in this way (Table 1).

### 3.3 Comparison and Uncertainty

Previous estimates of total N<sub>2</sub>O emissions over North America from TD approaches diverge in terms of magnitude and in terms of inter- and intra-annual variations. Saikawa et al. (2014) provided an estimate of 1.2±0.2 Tg N yr<sup>-1</sup> over North America between 2004 and 2008 using data from six measurement networks with extensive spatial coverage to constrain the global budget. Their estimates are in line with our ensemble [1.2 (0.9–1.4) Tg N yr<sup>-1</sup>] based on five TD estimates during the same period. Employing the posterior flux from the global atmospheric N<sub>2</sub>O inversion of Saikawa et al. (2014) as the standard prior, Nevison et al. (2018) estimated North American N<sub>2</sub>O emissions of 1.6±0.3 Tg N yr<sup>-1</sup> over 2008–2014 using the CarbonTracker-Lagrange (CT-L) regional inversion framework. The Midwestern Corn/Soybean Belt – an emission hot spot - accounted for 30% of total emissions from North America (Nevison et al., 2018), but this hot spot was weaker in the global inversions (Figure 3). In addition, Midwestern Corn/Soybean N<sub>2</sub>O emissions are elevated in spring and early summer owing to intensive N fertilizer applications and freeze-thaw dynamics (Nevison et al., 2018). Although the global and regional inversions had highest spring emissions, their amounts were obviously divergent (Figure S5). For example, PYVAR-CAMS and MIROC4-ACTM showed close spring N<sub>2</sub>O emissions to the CT-L regional inversion, while INVICAT and GEOS-Chem showed much lower emissions compared to CT-L. A number of factors may contribute to the large discrepancy in estimated N<sub>2</sub>O emissions between global inversion models and regional inversion (Nevison et al. 2018). First, the latter study used a substantially larger set of North American measurements, particularly NOAA aircraft data over the Midwest, especially with respect to MIROC4-ACTM (Tables S2 & S3). Second, the soil prior used in three global inversion models (PYVAR-CAMS, INVICAT, and GEOS-Chem) were from the model OCN-v.1.1 that showed a much lower spring N<sub>2</sub>O emissions from agricultural soils (Figures S6 & S7) and thus tended to shift the soil maximum away from spring and the Midwest. Third, the time frame of the global inversions (1995–2016) might dilute the impact of Midwestern sites like West Branch Iowa (WBI), which came online mid-2007, whereas the CT-L regional inversion focused on a subset of that period (2008–2015) that emphasized the impact of WBI (Table S3). Finally, the global inversions used much coarser resolution models [e.g., INVICAT (5.625°; at the scale of ~620km)] compared to CT-L at the spatial resolution of 1° (~111km) (Table S4). Thus, global models cannot reproduce

296 as well the small variations in atmospheric concentration and distribute the emissions more  
 297 diffusely in the Midwest Corn/Soybean belt extending from 36°N to 47°N (~1220km) and 102°  
 298 to 80°W (~2440km).

299 High N<sub>2</sub>O emission in the Midwestern Corn/Soybean Belt was also reported by all six  
 300 BU terrestrial biosphere models but to different degrees (Figure S7): DLEM and VISIT show  
 301 much higher emissions than the other four models (LPX-Bern, OCN, ORCHIDEE, and  
 302 ORCHIDEE-CNP). Seasonal N<sub>2</sub>O emissions from the BU models were highest in summer and  
 303 autumn (Figure S6), which differs from the regional (Nevison et al. 2018) and global inversions.  
 304 The lower spring N<sub>2</sub>O emissions estimated by BU models are probably associated with the  
 305 widely varied timing of N fertilizer application in each model and the omission of freeze-thaw  
 306 and wet-dry dynamics in some of model structure configurations.



307  
 308 **Figure 4.** Comparison of our anthropogenic N<sub>2</sub>O emissions from BU estimates with national  
 309 GHG inventories during 1990–2016: **a**, EPA; **b**, Canadian GHG inventory; **c**, Mexican GHG  
 310 inventory.

311 In addition, we compared anthropogenic N<sub>2</sub>O emissions from our BU approaches with  
 312 national inventories for the U.S., Canada, and Mexico during 1990–2016. There remain large  
 313 uncertainties in estimates from different BU approaches. Our total anthropogenic N<sub>2</sub>O emission  
 314 is on average 90 Gg N yr<sup>-1</sup> lower than that from the U.S. Environmental Protection Agency (EPA,  
 315 Figure 4a) 1990–2017 inventory reported in 2019, which is attributed to two times lower  
 316 inventory-based agricultural emissions from FAOSTAT, EDGARv4.3.2 and GAINS compared

317 to EPA and NMIP results (Figure S2a). The EPA 1990–2017 inventory of agricultural N<sub>2</sub>O  
318 emissions, which adopted a Tier3 approach based on the DayCent model for emissions from  
319 agricultural soils, is more consistent with our tier3, model-based (NMIP) estimates and trends.  
320 Recently, U.S. EPA extended anthropogenic N<sub>2</sub>O emissions to 2019. The estimate of  
321 anthropogenic N<sub>2</sub>O emissions in the 1990–2019 inventory increased by 20% compared to the  
322 1990–2017 inventory, which is due to a 21% higher estimate of agricultural soil emissions from  
323 the model improvement of freeze-thaw cycles in DayCent (Del Grosso, 2010, 2018) and a 330%  
324 higher estimate of waste emissions based on the revised domestic wastewater N<sub>2</sub>O methodology  
325 according to the IPCC 2019 Refinement (IPCC, 2019) (Figures 4a, S2a,d). When comparing  
326 agricultural N<sub>2</sub>O emissions, our NMIP results are on average 130 Gg N yr<sup>-1</sup> lower than the EPA  
327 1990–2019 inventory, consistent with the fact that some of NMIP models might underestimate  
328 agricultural soil N<sub>2</sub>O emissions due to missing freeze-thaw cycles. Our estimates of N<sub>2</sub>O  
329 emissions from fossil fuel and industry roughly agree with EPA-reported magnitudes and trends  
330 during 1990–2016 (Figures S2b, c).

331 By contrast, our total anthropogenic N<sub>2</sub>O emissions in Canada and Mexico, which reveal  
332 significant inter-annual variability, are on average 60 Gg N yr<sup>-1</sup> higher than estimates from the  
333 Canadian GHG inventory between 1990 and 2016 (Figure 4b) and the Mexican GHG inventory  
334 between 1990 and 2015 (Figure 4c), respectively. In both countries, NMIP agricultural emissions  
335 were twice as high as the four inventories (Figures S3a & S4a). Our estimates of N<sub>2</sub>O emissions  
336 from fossil fuel and industry showed a decrease during 1990–2016, and roughly agreed with the  
337 Canadian GHG inventory in terms of both magnitudes and trends (Figures S3b, c). Mexican  
338 industrial emissions of N<sub>2</sub>O (primarily from chemical production) increased by a factor of ~60  
339 since 1990, based on the estimate from EDGARv4.3.2 (Janssens-Maenhout et al. 2019),  
340 however, this massive increase was not observed in GAINS and the Mexican GHG inventory.  
341 Specifically, we found a threefold increase in industrial N<sub>2</sub>O emissions reported by GAINS  
342 (Winiwarter, 2005; Winiwarter et al., 2018), but a fourfold decrease by the Mexican GHG  
343 inventory during 1990–2010, and both inventories were almost equal thereafter until 2015  
344 (Figure S4b). The considerably large but uncertain contribution from Mexican industrial  
345 emissions over the recent decades reported by EDGARv4.3.2 needs more investigation.

346 Agriculture is the largest anthropogenic N<sub>2</sub>O emission source in the U.S. and Canada,  
347 owing to N inputs to cropland and pasture. Model-based direct soil N<sub>2</sub>O emissions showed a  
348 faster increasing trend with two times larger values compared with inventory-based estimates  
349 that were calculated based on the use of constant EFs (Figure S8). Along with rising N additions  
350 to agricultural soils (T. J. Griffis et al., 2017; Pärn et al., 2018; Smith, 1997; Tian et al., 2019),  
351 global warming may have elevated soil nitrification and denitrification processes, especially in  
352 boreal regions (e.g., Canada), thus also contributing to faster growth in N<sub>2</sub>O emissions. On the  
353 other hand, the assumed linear response of agricultural soil emissions to N fertilizer use may not  
354 realistically represent real-world emissions under varied climate and soil conditions (Shcherbak  
355 et al., 2014; Wang et al., 2019). The interactive effect between climate change and N additions as  
356 well as spatiotemporal variability in environmental factors such as rainfall and temperature can  
357 modulate the N<sub>2</sub>O yield from nitrification and denitrification. Moreover, EF-based inventories  
358 that fail to consider the legacy effect due to the long-term human-added N accumulation in soils  
359 may lead to an underestimate of agricultural soil N<sub>2</sub>O emissions (Thompson et al., 2019).

360        **3.4 Implications for Future Research**

361        Large uncertainties that remain in both TD and BU approaches need further  
 362 investigation. Inversion models are based on atmospheric N<sub>2</sub>O data measured by global and  
 363 regional monitoring networks and aircraft campaigns. Atmospheric inversions rely on a priori  
 364 estimates that may include inventory-based and model-based N<sub>2</sub>O emissions from natural and  
 365 agricultural soils, oceans, industry, and biomass burning (Nevison et al., 2018; Thompson et al.,  
 366 2014). For instance, we included two estimates from PYVAR-CAMS since two different ocean  
 367 prior fluxes were used. A high ocean prior flux used in PYVAR-CAMS-1 led to a low land flux.  
 368 In addition, more available measurement sites and expanded network coverage would improve  
 369 inversion accuracy. The estimates of the CT-L regional inversion were improved partially  
 370 because it uses a substantially larger set of North American measurements, particularly NOAA  
 371 aircraft data over the Midwest, and uses a higher resolution of the transport models compared  
 372 with global inversion models. Furthermore, more spatially accurate prior flux estimates will  
 373 improve confidence in the inversion results. BU estimates in our synthesis were not employed as  
 374 prior fluxes for the four inversion models. Moreover, the prior fluxes used in the four TD models  
 375 were from different data sources (Thompson et al., 2019). Future work should use the currently  
 376 synthesized BU estimates as a priori estimates in the TD framework to reconcile the inversions  
 377 with BU calculations. There remains large uncertainty in agricultural soil N<sub>2</sub>O emissions from  
 378 the process-based ecosystem models (Tian et al., 2019). First, this large uncertainty among  
 379 models is associated with different representations of biogeochemical processes and the omission  
 380 or simplification of agricultural practices. For instance, most NMIP models have not considered  
 381 the freeze-thaw cycle in soils. It has been reported that freeze-thaw cycles could contribute to  
 382 17%~28% more of global agricultural N<sub>2</sub>O emissions (Wagner-Riddle et al., 2017). The new  
 383 freeze-thaw version of DayCent model showed a 21% more N<sub>2</sub>O emission from U.S. agriculture  
 384 during 1990–2019 compared to its previous simulations, which was higher than NMIP results.  
 385 Second, model uncertainties in predicting cropland N<sub>2</sub>O emissions would be reduced through  
 386 improved representation of geospatial data and sub-national statistics to describe agricultural  
 387 practices more precisely like legume cultivation, rotation, tillage, and cover-crops. Third, NMIP  
 388 models' responses to different driving factors are divergent. Future research to improve accuracy  
 389 in model-based N<sub>2</sub>O emissions should include single-factor model validations against field  
 390 experiments.

391        **4 Conclusions**

392        North American N<sub>2</sub>O emissions estimated by BU approaches (1.7 Tg N yr<sup>-1</sup> during 2007–2016)  
 393 were on average 0.4 Tg N yr<sup>-1</sup> larger than the corresponding TD estimates in this study; however,  
 394 our mean BU estimate was roughly consistent with the CT-L regional inversion model in  
 395 Nevison et al. (2018). Anthropogenic emissions were the major contributor to the total North  
 396 American N<sub>2</sub>O source, and were dominated (68%) by agriculture and industry. Agriculture is the  
 397 largest overall N<sub>2</sub>O source and is attributable to soil N additions. The recent estimates from  
 398 NMIP and DayCent models showed that N<sub>2</sub>O directly emitted from agricultural soils has  
 399 exhibited a faster increase in recent years than predicted by EF-based national GHG inventories.  
 400 We speculate that EF-based inventories may underestimate agricultural N<sub>2</sub>O emissions due to  
 401 omission of interactive effects of environmental change and N additions, and legacy impacts of  
 402 long-term soil N accumulations. There remains uncertainty in TD and BU estimates of N<sub>2</sub>O at  
 403 both annual and seasonal time scales. For example, Nevison et al. (2018) emphasized that the

404 Midwestern Corn/Soybean Belt was a hotspot of N<sub>2</sub>O emission in North America, although this  
405 was not found with our global atmospheric inversions, albeit they all estimated above average  
406 emissions in the region. It is likely due to the smaller number of observations over the Midwest  
407 used in the global estimates, the longer time frame of global inversions that diluted the impact of  
408 Midwestern sites, and much coarser resolutions of transport models used in global inversions. On  
409 the other hand, high N<sub>2</sub>O emissions were simulated to different degrees in the Midwestern U.S.  
410 by the six BU terrestrial biosphere models used here.

411 We reported North American N<sub>2</sub>O emissions based on both TD and BU approaches and  
412 provided new insights into strengths and limitations of each approach for reducing future  
413 uncertainty. To reconcile the large divergence between TD and BU estimates, we recommend  
414 that more consistent and accurate prior fluxes, more available measurement sites, and expanded  
415 network coverage should be considered to improve the accuracy of atmospheric inversions.  
416 Meanwhile, improved representation and validation of biogeochemical processes (e.g., freeze-  
417 thaw and dry-wet cycles) and better geospatial data and statistics on agricultural practices (e.g.,  
418 legume cultivation, rotation, tillage, and cover-cropped system) could pave the way for better  
419 simulation of daily and cumulative soil N<sub>2</sub>O emissions.  
420

## 421 Acknowledgments

422 This research has been supported partly by NSF grant nos. 1903722, 1922687; NOAA grant nos.  
423 NA16NOS4780207 and NA16NOS4780204, Andrew Carnegie Fellowship Award no. G-F-19-  
424 56910. Additional funding support includes: R.L.T. and P.R. acknowledge funding support from  
425 VERIFY project (EC H2020 grant no. 776810). P.C. acknowledges support from ERC SyG  
426 GrantImbalance-P. P.C. and R.L. acknowledge support from the ANR Cland convergence  
427 institute. A.I. acknowledges funding support from JSPS KAKENHI grant (no. 17H01867). F.J.  
428 and S.L. acknowledge support by Swiss National Science Foundation (# #200020\_200511) and  
429 by the EC H2020 grant no. 821003 (Project 4C) and no. 820989 (Project COMFORT). The work  
430 reflects only the authors' view; the European Commission and their executive agency are not  
431 responsible for any use that may be made of the information the work contains. P.K.P. is partly  
432 supported by Environment Research and Technology Development Fund (#2-1802) of the  
433 Ministry of the Environment, Japan. K.C.W. and D.B.M. acknowledge support from NASA (IDS  
434 Grant #NNX17AK18G) and NOAA (Grant #NA13OAR4310086). P.A.R. acknowledges NASA  
435 Award NNX17AI74G. F.N.T. acknowledges funding from FAO regular programme. The views  
436 expressed in this publication are those of the author(s) and do not necessarily reflect the views or  
437 policies of FAO. S.Z. acknowledges support by the EC H2020 grant no. 647204. F.Z.  
438 acknowledges the support from the National Natural Science Foundation of China (41671464).  
439 We acknowledge Greet Janssens-Maenhout for providing EDGAR N<sub>2</sub>O emission data and  
440 Alexander F Bouwman for providing aquacultural N<sub>2</sub>O emission data. This work contributes to  
441 the REgional Carbon Cycle Assessment and Porcesses-2 of the Global Carbon Project. The  
442 relevant datasets of this study are archived in the box site at Auburn University  
443 (<https://auburn.box.com/s/csi2vkgrgcd267rxlvm97jnnccrx0hqi>).  
444

445 **References**

- 446 Beusen, A. H., Bouwman, A. F., Van Beek, L. P., Mogollón, J. M., & Middelburg, J. J. (2016). Global riverine N  
 447 and P transport to ocean increased during the 20th century despite increased retention along the aquatic  
 448 continuum. *Biogeosciences*, 13(8), 2441-2451.
- 449 Bouwman, A. F., Beusen, A., Overbeek, C., Bureau, D., Pawlowski, M., & Glibert, P. (2013). Hindcasts and future  
 450 projections of global inland and coastal nitrogen and phosphorus loads due to finfish aquaculture. *Reviews*  
 451 in *Fisheries Science*, 21(2), 112-156.
- 452 Chen, Z., Griffis, T. J., Millet, D. B., Wood, J. D., Lee, X., Baker, J. M., et al. (2016). Partitioning N<sub>2</sub>O emissions  
 453 within the US Corn Belt using an inverse modeling approach. *Global Biogeochemical Cycles*, 30(8), 1192-  
 454 1205.
- 455 Ciais, P., Sabine, C., Bala, G., Bopp, L., Brovkin, V., Canadell, J., et al. (2014). Carbon and other biogeochemical  
 456 cycles. In *Climate Change 2013: The Physical Science Basis. Contribution of Working Group I to the Fifth*  
 457 *Assessment Report of the Intergovernmental Panel on Climate Change* (pp. 465-570): Cambridge  
 458 University Press.
- 459 Dangal, S. R., Tian, H., Xu, R., Chang, J., Canadell, J. G., Ciais, P., et al. (2019). Global nitrous oxide emissions  
 460 from pasturelands and rangelands: Magnitude, spatio-temporal patterns and attribution. *Global*  
 461 *Biogeochemical Cycles*, 33, 200-222.
- 462 Del Grosso, S., Ogle, S., Parton, W., & Breidt, F. (2010). Estimating uncertainty in N<sub>2</sub>O emissions from US  
 463 cropland soils. *Global Biogeochemical Cycles*, 24(1).
- 464 Del Grosso, S. J. (2010). Grazing and nitrous oxide. *Nature*, 464(7290), 843-844. <https://doi.org/10.1038/464843a>
- 465 Del Grosso, S. J., Ogle, S. M., Parton, W. J., Nevison, C. D., Smith, W., Grant, B., et al. (2018). *Comparing soil*  
 466 *nitrous oxide emissions simulated by the new freeze-thaw version of daycent with fluxes inferred from*  
 467 *atmospheric inversion*. Paper presented at the AGU Fall Meeting Abstracts.
- 468 Du, E., de Vries, W., Han, W., Liu, X., Yan, Z., & Jiang, Y. (2016). Imbalanced phosphorus and nitrogen deposition  
 469 in China's forests. *Atmospheric Chemistry and Physics*, 16(13), 8571.
- 470 Eyring, V., Lamarque, J.-F., Hess, P., Arfeuille, F., Bowman, K., Chipperfield, M. P., et al. (2013). Overview of  
 471 IGAC/SPARC Chemistry-Climate Model Initiative (CCMI) community simulations in support of  
 472 upcoming ozone and climate assessments. 40(Januar), 48-66.
- 473 FAO. (2021). FAOSTAT, database of the Food and Agriculture Organization of the United Nations Statistics. Data  
 474 avaialble as follows:Livestock Manure: <http://www.fao.org/faostat/en/#data/EMN> ; Emissions totals:  
 475 <http://www.fao.org/faostat/en/#data/GT>; population: <http://www.fao.org/faostat/en/#data/OA>
- 476 FAO(2020). Livestock and environment statistics: manure and greenhouse gas emissions. Global, regional and  
 477 country trends, 1990–2018. FAOSTAT Analytical Brief Series No. 14. Rome.  
 478 <http://www.fao.org/3/cb1922en/cb1922en.pdf>
- 479 Griffis, T., Lee, X., Baker, J., Russelle, M., Zhang, X., Venterea, R., & Millet, D. (2013). Reconciling the  
 480 differences between top-down and bottom-up estimates of nitrous oxide emissions for the US Corn Belt.  
 481 *Global Biogeochemical Cycles*, 27(3), 746-754. <https://doi.org/10.1002/gbc.20066>
- 482 Griffis, T. J., Chen, Z., Baker, J. M., Wood, J. D., Millet, D. B., Lee, X., et al. (2017). Nitrous oxide emissions are  
 483 enhanced in a warmer and wetter world. *Proceedings of the National Academy of Sciences*, 114(45),  
 484 12081-12085. <https://doi.org/10.1073/pnas.1704552114>
- 485 Hurtt, G., Chini, L. P., Frolking, S., Betts, R., Feddema, J., Fischer, G., et al. (2011). Harmonization of land-use  
 486 scenarios for the period 1500–2100: 600 years of global gridded annual land-use transitions, wood harvest,  
 487 and resulting secondary lands. *Climatic Change*, 109(1-2), 117-161. DOI 10.1007/s10584-011-0153-2
- 488 IPCC. (2006). *2006 IPCC Guidelines for National Greenhouse Gas Inventories*. Retrieved from Hayama, Japan.
- 489 IPCC. (2019). *2019 Refinement to the 2006 IPCC Guidelines for National Greenhouse Gas Inventories*. Vol. 4  
 490 (IPCC, 2019).
- 491 Janssens-Maenhout, G., Crippa, M., Guizzardi, D., Muntean, M., Schaaf, E., Dentener, F., et al. (2019). EDGAR  
 492 v4.3.2 Global Atlas of the three major greenhouse gas emissions for the period 1970–2012. *Earth System*  
 493 *Science Data*, 11(3), 959-1002. <https://www.earth-syst-sci-data.net/11/959/2019/>
- 494 Kort, E. A., Eluszkiewicz, J., Stephens, B. B., Miller, J. B., Gerbig, C., Nehrkorn, T., et al. (2008). Emissions of CH<sub>4</sub>  
 495 and N<sub>2</sub>O over the United States and Canada based on a receptor-oriented modeling framework and  
 496 COBRA-NA atmospheric observations. *Geophysical Research Letters*, 35(18).  
 497 <https://doi.org/10.1029/2008GL034031>

- 498 Lauerwald, R., Regnier, P., Figueiredo, V., Enrich-Prast, A., Bastviken, D., Lehner, B., et al. (2019). Natural lakes  
 499 are a minor global source of N<sub>2</sub>O to the atmosphere. *Global Biogeochemical Cycles*, 33, 1564-1581.  
 500 <https://doi.org/10.1111/gcb.14928>
- 501 Lu, C., & Tian, H. (2017). Global nitrogen and phosphorus fertilizer use for agriculture production in the past half  
 502 century: shifted hot spots and nutrient imbalance. *Earth System Science Data*, 9(1), 181-192.  
 503 <https://doi.org/10.5194/essd-9-181-2017>
- 504 Maavara, T., Lauerwald, R., Laruelle, G. G., Akbarzadeh, Z., Bouskill, N. J., Van Cappellen, P., & Regnier, P.  
 505 (2019). Nitrous oxide emissions from inland waters: Are IPCC estimates too high? *Global Change Biology*,  
 506 25(2), 473-488.
- 507 MacLeod, M., Hasan, M. R., Robb, D. H. F., & Mamun-Ur-Rashid, M. (2019). *Quantifying and mitigating  
 508 greenhouse gas emissions from global aquaculture*. Retrieved from Rome.
- 509 McDaniel, M. D., Saha, D., Dumont, M., Hernández, M., & Adams, M. (2019). The effect of land-use change on  
 510 soil CH 4 and N 2 O fluxes: a global meta-analysis. *Ecosystems*, 22(6), 1424-1443.
- 511 Meurer, K. H., Franko, U., Stange, C. F., Dalla Rosa, J., Madari, B. E., & Jungkunst, H. F. (2016). Direct nitrous  
 512 oxide (N<sub>2</sub>O) fluxes from soils under different land use in Brazil—a critical review. *Environmental  
 513 Research Letters*, 11(2), 023001.
- 514 Miller, S., Kort, E., Hirsch, A., Dlugokencky, E., Andrews, A., Xu, X., et al. (2012). Regional sources of nitrous  
 515 oxide over the United States: Seasonal variation and spatial distribution. *Journal of Geophysical Research:  
 516 Atmospheres*, 117(D6).
- 517 Nevison, C., Andrews, A., Thoning, K., Dlugokencky, E., Sweeney, C., Miller, S., et al. (2018). Nitrous Oxide  
 518 Emissions Estimated With the Carbon Tracker-Lagrange North American Regional Inversion Framework.  
 519 *Global Biogeochemical Cycles*, 32(3), 463-485.
- 520 Pärn, J., Verhoeven, J. T., Butterbach-Bahl, K., Dise, N. B., Ullah, S., Aasa, A., et al. (2018). Nitrogen-rich organic  
 521 soils under warm well-drained conditions are global nitrous oxide emission hotspots. *Nature  
 522 Communications*, 9(1), 1135.
- 523 Patra, P. K., Takigawa, M., Watanabe, S., Chandra, N., Ishijima, K., & Yamashita, Y. (2018). Improved chemical  
 524 tracer simulation by MIROC4. 0-based atmospheric chemistry-transport model (MIROC4-ACM). *Sola*,  
 525 14, 91-96.
- 526 Prinn, R. G., Weiss, R. F., Arduini, J., Arnold, T., DeWitt, H. L., Fraser, P. J., et al. (2018). History of chemically  
 527 and radiatively important atmospheric gases from the Advanced Global Atmospheric Gases Experiment  
 528 (AGAGE). *Earth System Science Data*, 10(2), 985-1018. <https://www.earth-syst-sci-data.net/10/985/2018/>
- 529 Saikawa, E., Prinn, R., Dlugokencky, E., Ishijima, K., Dutton, G., Hall, B., et al. (2014). Global and regional  
 530 emissions estimates for N<sub>2</sub>O. *Atmospheric Chemistry and Physics*, 14, 4617-4641,  
 531 <https://doi.org/10.5194/acp-14-4617-2014>.
- 532 Shang, Z., Zhou, F., Smith, P., Saikawa, E., Ciais, P., Chang, J., et al. (2019). Weakened growth of cropland-N<sub>2</sub>O  
 533 emissions in China associated with nationwide policy interventions. *Global Change Biology*, 25(11), 3706-  
 534 3719. <https://onlinelibrary.wiley.com/doi/abs/10.1111/gcb.14741>
- 535 Shcherbak, I., Millar, N., & Robertson, G. P. (2014). Global metaanalysis of the nonlinear response of soil nitrous  
 536 oxide (N<sub>2</sub>O) emissions to fertilizer nitrogen. *Proceedings of the National Academy of Sciences*, 111(25),  
 537 9199-9204.
- 538 Smith, K. (1997). The potential for feedback effects induced by global warming on emissions of nitrous oxide by  
 539 soils. *Global change biology*, 3(4), 327-338.
- 540 Stehfest, E., & Bouwman, L. (2006). N<sub>2</sub>O and NO emission from agricultural fields and soils under natural  
 541 vegetation: summarizing available measurement data and modeling of global annual emissions. *Nutrient  
 542 Cycling in Agroecosystems*, 74(3), 207-228.
- 543 Thompson, R. L., Chevallier, F., Crotwell, A. M., Dutton, G. S., Langenfelds, R. L., Prinn, R. G., et al. (2014).  
 544 Nitrous oxide emissions 1999 to 2009 from a global atmospheric inversion. *Atmospheric Chemistry and  
 545 Physics*, 14, 1801-1817, <https://doi.org/10.5194/acp-14-1801-2014>.
- 546 Thompson, R. L., Lassaletta, L., Patra, P. K., Wilson, C., Wells, K. C., Gressent, A., et al. (2019). Acceleration of  
 547 global N<sub>2</sub>O emissions seen from two decades of atmospheric inversion. *Natural Climate Change*, 9, 993-  
 548 998.
- 549 Tian, H., Lu, C., Ciais, P., Michalak, A. M., Canadell, J. G., Saikawa, E., et al. (2016). The terrestrial biosphere as a  
 550 net source of greenhouse gases to the atmosphere. *Nature*, 531(7593), 225-228.  
 551 <https://doi.org/10.1038/nature16946>

- 552 Tian, H., Xu, R., Canadell, J. G., Thompson, R. L., Winiwarter, W., Suntharalingam, P., et al. (2020a). A  
 553 comprehensive quantification of global nitrous oxide sources and sinks. *Nature*, 586(7828), 248-256.  
 554 <https://doi.org/10.1038/s41586-020-2780-0>
- 555 Tian, H., Xu, R., Pan, S., Yao, Y., Bian, Z., Cai, W.-J., et al. (2020b). Long-Term Trajectory of Nitrogen Loading  
 556 and Delivery From Mississippi River Basin to the Gulf of Mexico. *Global Biogeochemical Cycles*, 34(5),  
 557 e2019GB006475. <https://doi.org/10.1029/2019GB006475>
- 558 Tian, H. Q., Yang, J., Xu, R. T., Lu, C. Q., Canadell, J. G., Davidson, E. A., et al. (2019). Global soil nitrous oxide  
 559 emissions since the preindustrial era estimated by an ensemble of terrestrial biosphere models: Magnitude,  
 560 attribution, and uncertainty. *Global Change Biology*, 25(2), 640-659.
- 561 Tubiello, F., Cónodor-Golec, R., Salvatore, M., Piersante, A., Federici, S., Ferrara, A., et al. (2015). *Estimating  
 562 greenhouse gas emissions in agriculture: a manual to address data requirements for developing countries.*  
 563 <http://www.fao.org/3/i4260e/i4260e.pdf>
- 564 Tubiello, F.N., 2019. GHG Emissions due to agriculture. *Encyclopedia of Food Security and Sustainability*, [Volume  
 565 1](#), 2019, Pages 196-205, <https://doi.org/10.1016/B978-0-08-100596-5.21996-3>
- 566 Van Der Werf, G. R., Randerson, J. T., Giglio, L., Van Leeuwen, T. T., Chen, Y., Rogers, B. M., et al. (2017).  
 567 Global fire emissions estimates during 1997-2016. *Earth System Science Data*, 9, 697-720.
- 568 van Lent, J., Hergoualc'h, K., & Verchot, L. V. (2015). Reviews and syntheses: Soil N<sub>2</sub>O and NO emissions from  
 569 land use and land-use change in the tropics and subtropics: a meta-analysis. *Biogeosciences*, 12(23), 7299-  
 570 7313.
- 571 Verchot, L. V., Davidson, E. A., Cattâniao, H., Ackerman, I. L., Erickson, H. E., & Keller, M. (1999). Land use  
 572 change and biogeochemical controls of nitrogen oxide emissions from soils in eastern Amazonia. *Global  
 573 Biogeochemical Cycles*, 13(1), 31-46.  
 574 <https://agupubs.onlinelibrary.wiley.com/doi/abs/10.1029/1998GB900019>
- 575 Wagner-Riddle, C., Congreves, K. A., Abalos, D., Berg, A. A., Brown, S. E., Ambadan, J. T., et al. (2017). Globally  
 576 important nitrous oxide emissions from croplands induced by freeze-thaw cycles. *Nature Geoscience*,  
 577 10(4), 279-283. <https://doi.org/10.1038/ngeo2907>
- 578 Wang, Q., Zhou, F., Shang, Z., Ciais, P., Winiwarter, W., Jackson, R. B., et al. (2019). Data-driven estimates of  
 579 global nitrous oxide emissions from croplands. *National Science Review*, 00, 1-12.
- 580 Wells, K. C., Millet, D. B., Bouscerez, N., Henze, D. K., Chaliyakunnel, S., Griffis, T. J., et al. (2015). Simulation of  
 581 atmospheric N<sub>2</sub>O with GEOS-Chem and its adjoint: evaluation of observational constraints.  
 582 *Geosci. Model Dev.*, 8(10), 3179-3198. <https://www.geosci-model-dev.net/8/3179/2015/>
- 583 Williams, J., & Crutzen, P. J. (2010). Nitrous oxide from aquaculture. *Nature Geoscience*, 3, 143. Correspondence.  
 584 <https://doi.org/10.1038/ngeo804>
- 585 Wilson, C., Chipperfield, M., Gloor, M., & Chevallier, F. (2014). Development of a variational flux inversion  
 586 system (INVICAT v1. 0) using the TOMCAT chemical transport model. *Geoscientific Model Development*,  
 587 7, 2485-2500.
- 588 Winiwarter, W. (2005). The GAINS model for greenhouse gases-version 1.0: nitrous oxide (N<sub>2</sub>O).
- 589 Winiwarter, W., Höglund-Isaksson, L., Klimont, Z., Schöpp, W., & Amann, M. (2018). Technical opportunities to  
 590 reduce global anthropogenic emissions of nitrous oxide. *Environmental Research Letters*, 13(1), 014011.
- 591 Xu, R., Tian, H., Pan, S., Dangal, S. R., Chen, J., Chang, J., et al. (2019). Increased nitrogen enrichment and shifted  
 592 patterns in the world's grassland: 1860–2016. *Earth System Science Data*, 11(1), 175-187.
- 593 Xu, X., Tian, H., Chen, G., Liu, M., Ren, W., Lu, C., & Zhang, C. (2012). Multifactor controls on terrestrial N<sub>2</sub>O  
 594 flux over North America from 1979 through 2010. *Biogeosciences*, 9(4), 1351-1366.
- 595 Yao, Y., Tian, H., Shi, H., Pan, S., Xu, R., Pan, N., & Canadell, J. G. (2020). Increased global nitrous oxide  
 596 emissions from streams and rivers in the Anthropocene. *Natural Climate Change*, 10(2), 138-142.
- 597 Zaehle, S., Ciais, P., Friend, A. D., & Prieur, V. (2011). Carbon benefits of anthropogenic reactive nitrogen offset by  
 598 nitrous oxide emissions. *Nature Geoscience*, 4, 601-605.
- 599 Zhang, B., Tian, H., Lu, C., Dangal, S. R., Yang, J., & Pan, S. (2017). Global manure nitrogen production and  
 600 application in cropland during 1860–2014: a 5 arcmin gridded global dataset for Earth system modeling.  
 601 *Earth System Science Data*, 9(2).
- 602
- 603
- 604
- 605